Growth and optical properties of Er^{3+}-doped $BaGd_2(MoO_4)_4$ crystal

Shujuan HAN – Key Laboratory of Functional Materials and Devices for Special Environments, Xinjiang Technical Institute of Physics & Chemistry, Chinese Academy of Sciences, State Key Laboratory of Crystal Materials, Shandong University, Jinan 250100, China; Jiyang WANG, Huaijin ZHANG – State Key Laboratory of Crystal Materials, Shandong University, Jinan 250100, China; Shilie PAN – Key Laboratory of Functional Materials and Devices for Special Environments, Xinjiang Technical Institute of physics & Chemistry, Chinese Academy of Sciences; Honghao XV, Yicheng WANG, Chuanying SHEN – State Key Laboratory of Crystal Materials, Shandong University, Jinan 250100, China

Please cite as: CHEMIK 2013, **67**, 9, 763–770

Introduction

With the development of high power diode lasers, there has been increasing research interest in diode pumped solid-state laser materials [1÷3]. It is well-known that, Er^{3+} is a suitable diode-pumped laser ion with optical transitions in the infrared region as well as in the visible wavelength range. Er^{3+} ions can emit 1.55μm fluorescence through the $^4I_{13/2} \rightarrow {}^4I_{15/2}$ transition. The infrared emission of Er^{3+} around 1.55μm has gained the attention of researchers due to its important applications in laser radar, eye-safe light detection, optical communications and the medical field [4÷7]. Therefore, Er^{3+}-doped crystal materials have been widely investigated.

Monoclinic double molybdate crystals with the formula $BaRe_2(MoO_4)_4$ (Re = rare earth) were investigated as host materials for solid-state lasers. The $BaGd_2(MoO_4)_4$ crystal has a perfect (010) cleavage plane, and the cleavage character makes the crystal suitable as a gain medium for microchip lasers because it can be easily cleaved into wafers with sub-millimeter thickness [8]. In previous work, spectroscopic characterization was made and 1.06 μm laser operation was demonstrated in Nd^{3+}: $BaGd_2(MoO_4)_4$ [9, 10]. Laser performance has also been demonstrated in Tm^{3+} and Yb^{3+}: $BaGd_2(MoO_4)_4$ crystals [8, 11]. In addition, we reported on the growth and spectroscopic characterization of $BaNd_2(MoO_4)_4$ crystals [12].

In this paper, we report on the crystal growth and spectroscopic characterization of Er^{3+}: $BaGd_2(MoO_4)_4$. In this work, the concentration of Er^{3+} is at about a 1% at substitution level for Gd^{3+}.

2. Experimental

2.1. Crystal growth

Since the $BaGd_2(MoO_4)_4$ crystal melts congruently, the Er^{3+}: $BaGd_2(MoO_4)_4$ crystal can be grown by the Czochralski method using a platinum crucible that is 70 mm in diameter and 40 mm in height. The heating apparatus is a 2 kHz intermediate frequency furnace that was used to heat the crucible.

Polycrystalline Er^{3+}: $BaGd_2(MoO_4)_4$ material was synthesized by a solid-phase reaction with 99.99% pure Er_2O_3, $BaCO_3$, Gd_2O_3 and MoO_3. The raw materials, with composition $BaEr_{0.02}Gd_{1.98}(MoO_4)_4$, were weighed. A 1.5 wt% excess amount of MoO_3 was added to the mixture to compensate for the volatilization of MoO_3 during synthesis of the polycrystal and crystal growth. The weighed materials were ground, mixed and heated at 800°C for 12 h in a platinum crucible. After the crucible cooled down to room temperature, the mixture was remixed, pressed into pellets and reheated at 850°C for 12 h to allow the polycrystalline compounds to react completely.

Initially, a Pt wire with 0.5 mm diameter was used as a crystal seed. Then a seed cut from the crystal grown with the Pt wire seed was used to grow a large sized single crystal. The pulling rate was varied from 0.7 to 2 mm/h and the crystal rotation speed was kept between 6 and 8 rpm. After growth was completed, the crystal was cooled to room temperature at a rate of 10 °C/h. The Er^{3+}: $BaGd_2(MoO_4)_4$ crystal tends to crack during the annealing process due to spontaneous cleavage. Figure 1 shows the unpolished cleaved microchips that were obtained.

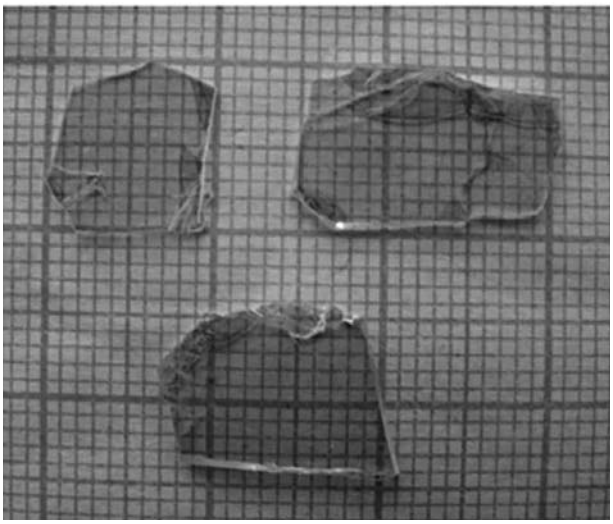

Fig. 1. Cleaved microchip without polishing of Er^{3+}: $BaGd_2(MoO_4)_4$

2.2. Effective segregation coefficient

X-ray fluorescence analysis was used to measure the concentration of elemental Er, Ba, Gd, and Mo in the crystal. The specimen measured was cut from the as-grown crystal and ground into powder. The polycrystalline material used for growing the crystal was referenced as a comparison standard. Based on the measurement results, the effective segregation coefficients of Er, Ba, Gd, and Mo in the grown crystal were calculated.

2.3. Specific heat measurement

Specific heat was measured using a differential scanning calorimeter (NETZSCH model STA 449C) over the temperature range of 25–300°C at a heating rate of 5°C/min.

2.4. Absorption spectrum measurement

The absorption spectrum was recorded on a Jasco model V-570 UV/visible/ near IR spectrophotometer over the range of 200–1800 nm at room temperature.

2.5. Fluorescence spectrum and fluorescence decay curves measurement

The fluorescence spectrum was measured using Xenon lamp excitation over the range of 850–1700 nm at room temperature. The excitation wavelength was 522 nm. The fluorescence decay curves at 1536 and 998 nm, corresponding to the respective transitions $^4I_{13/2} \rightarrow {}^4I_{15/2}$ and $^4I_{11/2} \rightarrow {}^4I_{15/2}$, were measured.

3. Results and discussion

3.1. Doped concentration

The effective segregation coefficients k of Er^{3+}, Ba^{2+}, Gd^{3+}, and Mo^{6+} in the Er^{3+}: $BaGd_2(MoO_4)_4$ crystal was calculated using the equation $k = c_1/c_2$, where c_1 and c_2 are the respective concentrations of the ions in the crystal and raw materials. The effective segregation coefficients of Er^{3+}, Ba^{2+}, Gd^{3+}, and Mo^{6+} are determined to be 0.973, 0.988, 1.039, 0.966, respectively.

3.2. Specific heat

Specific heat is an important factor that influences the damage threshold of laser crystals. It is generally expected that a material with higher specific heat will have more resistance to laser damage. The dependence of the specific heat of the obtained crystal on temperature is shown in Figure 2. From this Figure, we can see that the specific heat increases almost linearly with temperature, and it ranges from 0.471 to 0.642 J g^{-1} K^{-1} over the temperature range from 25 to 300°C. The specific heat is 0.502 J g^{-1} K^{-1} at 50°C, a value that is slightly larger than that of Nd^{3+}:$BaGd_2(MoO_4)_4$ [9] and Er^{3+}:$LiLa(MoO_4)_2$, and slightly lower than that of Er^{3+}:$NaY(MoO_4)_2$ [6]. Therefore, Er^{3+}:$BaGd_2(MoO_4)_4$ should exhibit a higher laser damage threshold than Nd^{3+}:$BaGd_2(MoO_4)_4$ and Er^{3+}:$LiLa(MoO_4)_2$ and a lower one than Er^{3+}:$NaY(MoO_4)_2$.

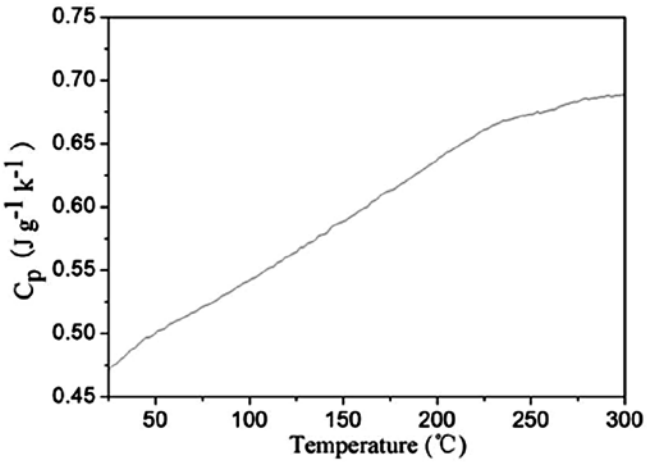

Fig. 2. Dependence of the specific heat of Er^{3+}: $BaGd_2(MoO_4)_4$ on temperature

3.3. Optical spectrum analysis

The absorption spectrum of the Er^{3+}: $BaGd_2(MoO_4)_4$ crystal is shown in Figure 3. The profile of the absorption spectrum is similar to that of other Er^{3+}-doped crystals, such as Er^{3+}: $Sr_3Y(BO_3)_3$ [4], Er^{3+}:$LiLa(MoO_4)_2$ [6], and Er^{3+}:$LiGd(MoO_4)_2$ [7]. From this Figure, it is observed that there are several absorption peaks from 360 to 1800 nm. The wavelengths centre at 380, 452, 490, 522, 656, 802, 980 and 1534 nm. They respectively relate to transitions from the Er^{3+} ground states, $^4I_{15/2}$, to the excited states $^4G_{11/2}$, $^4F_{5/2}$ + $^4F_{3/2}$, $^4F_{7/2}$, $^2H_{11/2}$, $^4F_{9/2}$, $^4I_{9/2}$, $^4I_{11/2}$ and $^4I_{13/2}$. The interesting feature in the absorption spectrum is the strong broad absorption band with a full width at half maximum (FWHM) of about 13 nm at 522 nm and of 10 nm at 380 nm. As a consequence, the pumping wavelength was chosen to be 522 nm.

Upon excitation of the Er^{3+}: $BaGd_2(MoO_4)_4$ crystal at 522 nm, the luminescence emission spectrum of the crystal was measured and is shown in Figure 4. From this Figure, it can be seen that the emission intensity at 1450-1600 nm corresponding to the $^4I_{13/2} \rightarrow ^4I_{15/2}$ transition is stronger than that in the wavelength range 950-1000 nm corresponding to the $^4I_{11/2} \rightarrow ^4I_{15/2}$ transition. The most intense emission band at 1536 nm, can potentially be used for eye-safe lasers. It also can be found that there are small peaks near 1536 nm, which is the result of energy levels splitting of Er^{3+} ion because of the effect of crystal field.

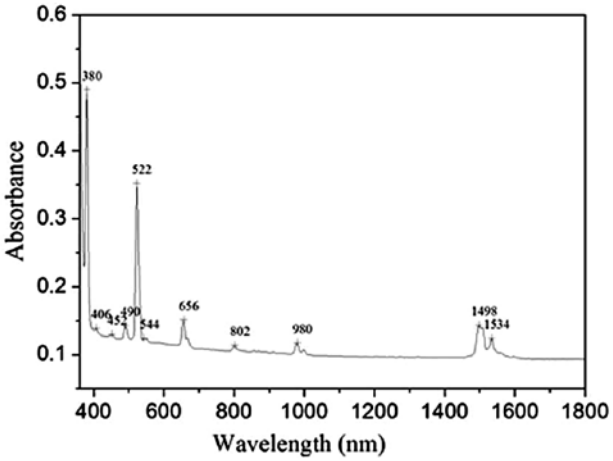

Fig. 3. Absorption spectrum of Er^{3+}: $BaGd_2(MoO_4)_4$ at room temperature

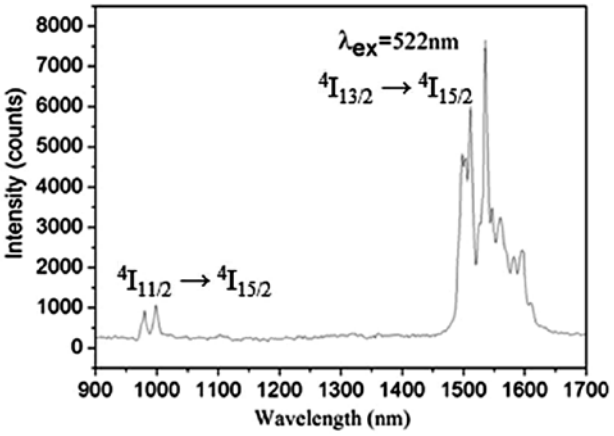

Fig. 4. Fluorescence spectrum of Er^{3+}: $BaGd_2(MoO_4)_4$ at room temperature

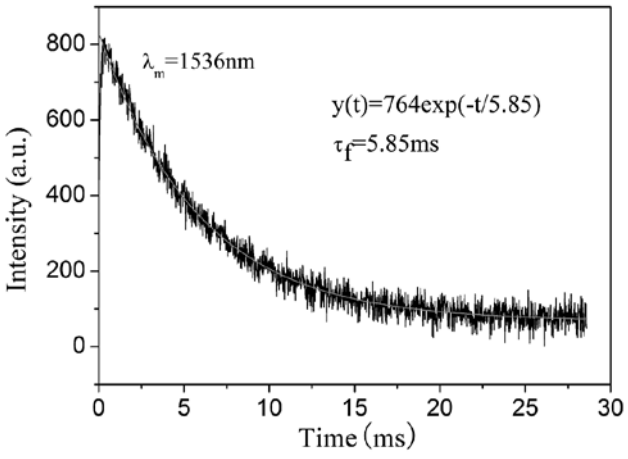

Fig. 5. Fluorescence decay curves of Er^{3+}: $BaGd_2(MoO_4)_4$ at 1536 nm

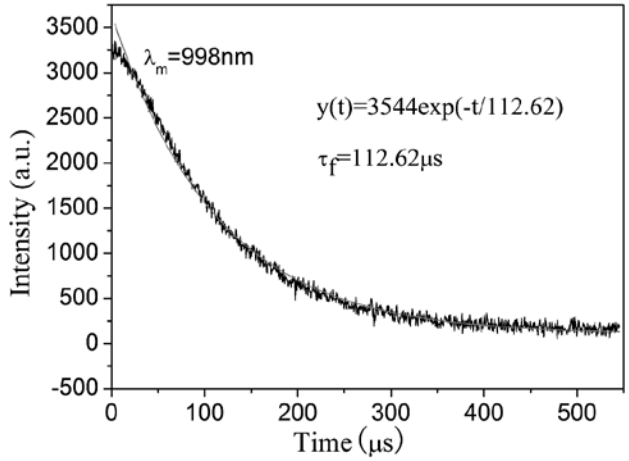

Fig. 6. Fluorescence decay curves of Er^{3+}: $BaGd_2(MoO_4)_4$ at 998 nm

The fluorescence lifetime of the $^4I_{13/2}\rightarrow{}^4I_{15/2}$ transition of Er^{3+}: $BaGd_2(MoO_4)_4$ at room temperature is shown in Figure 5. The lifetime (5.85 ms) determined by fitting to a single exponential is longer than the radiative lifetime (4.89 ms) seen from Table 2. This phenomenon has also existed in some other Er^{3+}-doped hosts, such as Er^{3+}:$NaGd(WO_4)_2$ [13], Er^{3+}:$NaY(MoO_4)_2$ [14], Er^{3+}:$LiNbO_3$[15]. This may be resulted from excitation trapping and emission reabsorption [16, 17].

The fluorescence decay curve at 998 nm for Er^{3+}: $BaGd_2(MoO_4)_4$ is shown in Figure 6. The lifetime of the $^4I_{11/2}\rightarrow{}^4I_{15/2}$ transition of the crystal was measured to be 112.62 μs, which is close to the corresponding value for Er^{3+}:$LiGd(MoO_4)_2$ [7].

3.4. Judd–Ofelt analysis

Judd–Ofelt theory is the most effective theory for the analysis of optical properties of rare earth ions doped in the crystals and glasses [18].

The integrated absorption coefficient $\int K(\lambda)d\lambda$, the transition-line intensity $S_{exp}(J\rightarrow J')$, the oscillator strength for the absorption $P_{exp}(J\rightarrow J')$ and the differential absorption cross section $\sigma_a(\lambda)$ may be written [19]

$$\sigma_a(\lambda)=\frac{D(\lambda)}{N_0 L\lg e} \tag{1}$$

$$\int K(\lambda)d\lambda = N_0\frac{8\pi^3 e^2\bar{\lambda}}{3hc}\frac{(n^2+2)^2}{9n}\frac{1}{(2J+1)}S_{\exp}(J\rightarrow J') = N_0\frac{\pi\bar{\lambda}^2e^2}{mc^2}P_{\exp}(J\rightarrow J') \tag{2}$$

Where l is the thickness of the sample, e is the electron charge, D(λ) is the absorbance, (J→J′) represents the transition from the ground multiplet 4I15/2 to an excited J′-multiplet, n is the refractive index of the crystal, c is the speed of light, h is Planck's constant, m is the electron mass, N_0 is the average Er3+ in the lattice structure. Owing to the cleavage nature of the $BaGd_2(MoO_4)_4$, it is difficult to measure its refractive index and then obtain its Sellmeier equations. So, an approximate refractive index of 2.02 is generally adopted for the $BaGd_2(MoO_4)_4$ crystal in spectral analysis [10]. Line intensities and optical parameters of Er^{3+}: $BaGd_2(MoO_4)_4$ crystal are listed in Table 1.

Table 1

Line intensities and optical parameters of the Er^{3+}: $BaGd_2(MoO_4)_4$ crystal

Transition final state $4f''\psi''j''$	Central wavelength (nm)	σ_a ($\times10^{-20}cm^2$)	$\int K(\lambda)d\lambda$ ($\times10^{-7}$)	$S_{exp}(J\rightarrow J')$ ($\times10^{-20}cm^2$)	$P_{exp}(J\rightarrow J')$ ($\times10^{-6}cm^2$)
$^4G_{11/2}$	380	7.6172	45.3436	16.6101	59.3047
$^2H_{9/2}$	407	0.2045	1.1394	0.3897	1.2991
$^4F_{3/2},{}^4F_{5/2}$	452	0.1534	1.1303	0.3481	1.0449
$^4F_{7/2}$	490	0.9623	0.5349	0.1519	0.4207
$^2H_{11/2}$	522	6.328	38.3557	10.2282	26.5845
$^4S_{3/2}$	544	0.1749	1.345	0.3441	0.8583
$^4F_{9/2}$	656	1.1932	6.5789	1.3960	2.8873
$^4I_{9/2}$	802	0.2404	1.4457	0.2509	0.4245
$^4I_{11/2}$	980	0.4603	4.6177	0.6559	0.9080
$^4I_{13/2}$	1498	1.109	19.1011	1.7749	1.6076

According to the J-O theory, the line strength of the electric-dipole transitions can also be expressed as

$$S_{cal}(J''\rightarrow J') = \sum_{t=2,4,6}\Omega_t\left|\langle 4f^n\psi''J''\|U^{(t)}\|4f^n\psi'J'\rangle\right|^2 \tag{3}$$

Where $U^{(t)}$ (t=2, 4 and 6) are the matrix elements of unit tensor operators and their values can be found from [20-21]. By a least-root-mean-square fitting between Eqs. (2) and (3), the J-O intensity parameters Ω_t (t=2, 4 and 6) were obtained and fitted as $\Omega_2=15.66465\times10^{-20}cm^2$, $\Omega_4=1.82670\times10^{-20}cm^2$, $\Omega_6=0.89712\times10^{-20}cm^2$.

Given Ω_t (t=2, 4 and 6), the radiative lifetime of a given upper level and the branching ration of the fluorescence emission can also be calculated

$$A(J''\rightarrow J') = \frac{64\pi^4e^2}{3h\bar{\lambda}^3}\frac{n(n^2+2)^2}{9}\frac{1}{(2J''+1)}S_{cal}(J''\rightarrow J') \tag{4}$$

$$\tau_{rad}=\frac{1}{\sum_{J'}A(J''\rightarrow J')} \tag{5}$$

$$\beta_{J''J'}=\frac{A(J''\rightarrow J')}{\sum_{J'}A(J''\rightarrow J')} \tag{6}$$

The calculated results are given in Table 2. The stimulated emission cross section σ_{em} can be calculated from

$$\sigma_{em}=\frac{\lambda^4}{8\pi\cdot c\cdot n^2\cdot\Delta\lambda\cdot\tau_r} \tag{7}$$

Where λ is the wavelength of the fluorescence peak, n is the refractive index, Δλ is the frequency FWHM. The stimulated emission cross section at about 1536 nm for the transition $^4I_{13/2}\rightarrow{}^4I_{15/2}$ is $4.50\times10^{-20}cm^2$, which is beneficial to the realization of human security of the laser output.

Table 2

Luminescence parameters of the Er^{3+}: $BaGd_2(MoO_4)_4$ crystal

	Final state	Radiation (nm)	$S_{cal}(J''\rightarrow J')$ ($\times10^{-20}cm^2$)	$P_{cal}(J''\rightarrow J')$ ($\times10^{-6}cm^2$)	$A(J''\rightarrow J')$ (S^{-1})	τ_{rad} (ms)	β_{TT} (%)	$\sum(J''\rightarrow J')$ ($\times10^{-18}cm^2$)
$^4I_{13/2}$	$^4I_{15/2}$	1536	1.8040	6.2449	204.484	4.89	100	1.6046
$^4I_{11/2}$	$^4I_{13/2}$	2777.8	1.8051	1.1753	40.5168	2.296	9.3029	1.0371
	$^4I_{15/2}$	998	0.7969	1.4557	395.0111		90.697	1.2846
	$^4I_{11/2}$	4651.2	0.2841	0.1326	1.6305		0.3691	0.1170
$^4I_{9/2}$	$^4I_{13/2}$	1739.1	0.6681	0.8338	73.3470	2.263	16.6019	0.7359
	$^4I_{15/2}$	800	0.3253	0.8824	366.8199		83.0289	0.7788
	$^4I_{9/2}$	3508.8	2.0395	1.2615	27.2561		0.8574	1.1132
$^4F_{9/2}$	$^4I_{11/2}$	1980.2	2.2750	2.4935	169.1542	0.315	5.3212	2.2004
	$^4I_{13/2}$	1156.1	0.5023	0.9429	187.6696		5.9036	0.8321
	$^4I_{15/2}$	660.1	1.3924	4.5779	2794.794		87.9177	4.0398
	$^4F_{9/2}$	3125	0.0242	0.0421	1.1462		0.0432	0.0371
	$^4I_{9/2}$	1639.3	0.3719	1.2314	121.8919		4.6035	1.0866
$^4S_{3/2}$	$^4I_{11/2}$	1212.1	0.0740	0.3312	59.9588	0.3776	2.2644	0.2922
	$^4I_{13/2}$	863.6	0.3106	1.9516	696.0757		26.2886	1.7222
	$^4I_{15/2}$	545	0.1983	1.9750	1768.75		66.8002	1.7428

4. Conclusions

An Er^{3+}: $BaGd_2(MoO_4)_4$ single crystal was grown by the Czochralski method. A spectroscopic characterization of the crystal was made. There are several strong absorption peaks over the range from 380 to 1600 nm and intense fluorescence peaks were observed. The intensity at 1450-1600 nm, attributed to the $^4I_{13/2} \rightarrow {}^4I_{15/2}$ transition, is much larger than that at 950-1000 nm attributed to the $^4I_{11/2} \rightarrow {}^4I_{15/2}$ transition. The fluorescence lifetime of $^4I_{13/2}$ and $^4I_{11/2}$ is around 5.85 ms and 112.62 μs, respectively. The results reveal that the Er^{3+}: $BaGd_2(MoO_4)_4$ crystal can be regarded as a potential laser material.

Acknowledgments

This work is supported by the Western Light of Chinese Academy of Sciences (Grant No. XBBS201220), National Key Basic Research Program of China (Grant No. 2012CB626803), the "National Natural Science Foundation of China" (Grant Nos. U1129301, 51172277, 21101168, 11104344), Main Direction Program of Knowledge Innovation of Chinese Academy of Sciences (Grant No. KJCX2-EW-H03-03), the "One Hundred Talents Project Foundation Program" of Chinese Academy of Sciences, Major Program of Xinjiang Uygur Autonomous Region of China during the 12th Five-Year Plan Period (Grant No. 201130111), the "High Technology Research and Development Program" of Xinjiang Uygur Autonomous Region of China (Grant No. 201116143).

Literature

1. J. Li, G.G. Xu, S.J. Han, J.D. Fan, J.Y. Wang, J. Cryst. Growth. 311 (2009) 4251.
2. G. Boulon, G. Metrat, N. Muhlstein, A. Brenier, M.R. Kokta, L. Kravchik, Y. Kalisky, Opt. Mater. 24 (2003) 377.
3. A.S. Kumaran, S.M. Babu, S. Ganesamoorthy, I. Bhaumik, A.K. Karanal, J. Cryst. Growth. 292 (2006) 368.
4. D. Zhao, G.F. Wang, J. Lumin. 130 (2010) 424.
5. J. Li, J.Y. Wang, H. Tan, H.J. Zhang, F. Song, S. Zhao, J.X. Zhang, X.X. Wang, Mater. Res. Bull. 39 (2004) 1329.
6. X.Y. Huang, G.F. Wang, J. Alloys Compd. 475 (2009) 693.
7. X.Y. Huang, W. Zhao, G.F. Wang, X.X. Li, Q.M. Yu, J. Alloys Compd. 509 (2011) 6578.
8. H.M. Zhu, Y.J. Chen, Y.F. Lin, X.H. Gong, Z.D. Luo, Y.D. Huang, J. Opt. Soc. Am. B 25 (2008) 801.
9. D. Zhao, Z.B. Lin, L.Z. Zhang, G.F. Wang, J. Phys. D: Appl. Phys. 40 (2007) 1018.
10. H.M. Zhu, Y.J. Chen, Y.F. Lin, X.H. Gong, Z.D. Luo, Y.D. Huang, Appl Phys B. 93 (2008) 429.
11. H.M. Zhu, Y.J. Chen, X.H. Gong, Q.G. Tan, Z.D. Luo, Y.D. Huang , J Appl Phys. 101 (2007) 063109.
12. S.J. Han, J.Y. Wang, J. Li, Y.J. Guo, Y.Z. Wang, L.L. Zhao, J. Lumin. 131 (2011) 244.
13. J.H. Huang, X.H. Gong, Y.J. Chen, Y.F. Lin, Q.G. Tan, Z.D. Luo, et al., Mater. Lett. 61 (2007) 3400.
14. X.Z. Li, Z.B. Lin, L.Z. Zhang, G.F.Wang, J. Cryst. Growth. 293 (2006) 157.
15. J. Amin, B. Dussardier, T. Schweizer, M. Hempstead, J. Lumin. 69 (1996) 17.
16. K.A. Subbotin, E.V. Zharikov, V.A. Smirnov, Opt. Spectrosc. 92 (2002) 601.
17. D.S. Sumida, T.Y. Fan, Opt. Lett. 19 (1994) 1343.
18. B.R. Judd, Phys. Rev. 127 (1962) 750.
19. W.F. Krupke, Phys. Rev. 145 (1966) 325.
20. A.A. Kaminskii, Crystalline Lasers: Physical Processes and Operating Schemes, CRC Press, Boca Raton, FL, 1996, p. 243.
21. P. Goldner, F. Auzel, J. Appl. Phys. 79 (1996) 7972.

Shujuan HAN – Ph.D., graduated from the State Key Laboratory of Crystal Materials, Shandong University, Jinan, China. Her doctoral thesis (Growth Exploration and Properties of Molybdate and Borate crystals) was awarded in 2012. She currently works for Key Laboratory of Functional Materials and Devices for Special Environments, Xinjiang Technical Institute of physics & Chemistry, Chinese Academy of Sciences. Research interests: Crystal growth and characterizations, exploration of the new nonlinear optical crystals.

e-mail:shujuanhan84@163.com, phone: +86 991 367 45 58

Jiyang WANG – Professor, doctorial tutor, graduated from Department of Chemistry, Nanjing University, Nanjing, China(1968). He currently works for State Key Laboratory of Crystal Materials, Shandong University, Jinan, China. Research interests: Functional crystal growth by flux and Czocchraski methods, and their characterization and applications. More than 20 different kinds of crystals have been successfully grown in his group including KTiOPO4(KTP) family, $KTiOPO_4$(KTP), $KBeBO_3F$(KBBF), $KAl_2B_2O_7$(KABO), NdP_5O1_4, PrP_5O1_4, family ErP_5O1_4, $NdAl_3(BO_3)_4$(NAB), NdxY1-$xAl_3(BO_3)_4$(NYAB), YbxY1-$xAl_3(BO_3)_4$(Yb:YAB), family NdxGd1-$xAl_3(BO_3)$ (NGAB), $GdCa_4O(BO_3)_3$, (GdCOB), $YCa_4O(BO_3)_3$, family (YCOB), YVO_4, $GdVO_4$, family $LuVO_4$, $KY(WO_4)_2$, $KGd(WO_4)_2$, family $KLu(WO_4)_2$, $BaWO_4$, crystals, stoichometric $LiNbO_3$ and $La_3Ga_5SiO1_4$ crystals for electrooptical applications.

e-mail: jywang@sdu.edu.cn, phone: +86 0531 883 643 40

Huaijin ZHANG – Professor, doctorial tutor, graduated from Department of Physics, Shandong University, Jinan, China. He currently works for State Key Laboratory of Crystal Materials, Shandong University, Jinan, China. Research interests: Material science(crystal growth, Czmethod, FZ method); Laser crystals, Nonlinear crystals, Piezoelectric (ferroelectric) crystals and so on.

e-mail: huaijinzhang@sdu.edu.cn, phone: + 86 0531 883 646 86

Shilie PAN – Professor, doctorial tutor, received his Ph.D. from University of Science & Technology of China in 2002. He currently works for Key Laboratory of Functional Materials and Devices for Special Environments, Xinjiang Technical Institute of physics & Chemistry, Chinese Academy of Sciences. He mainly engages in research and development of new nonlinear optical materials (new frequency-doubling materials and new electro-optic materials), new piezoelectric materials, new ferroelectric materials, and their device applications.

e-mail:slpan@ms.xjb.ac.cn, phone: +86 991 367 45 58

Honghao XV – doctoral student, is studying at State Key Laboratory of Crystal Materials, Shandong University, Jinan, China. Research interests: Laser crystal growth and characterizations.

e-mail: xuhonghao1234@126.com@sdu.edu.cn, phone: +86 0531 883 664 32

Yicheng WANG – doctoral student, is studying at State Key Laboratory of Crystal Materials, Shandong University, Jinan, China. Research interests: Laser crystal growth and characterizations.

e-mail: elbarwon@gmail.com, phone: +86 0531 883 664 32

Chuanying SHEN – doctoral student, is studying at State Key Laboratory of Crystal Materials, Shandong University, Jinan, China. Research interests: crystal growth and characterizations.

e-mail: shenshouchuan@163.com, phone: +86 0531 883 664 32